Analysis of variations in ocean color[1]

André Morel and Louis Prieur

Laboratoire de Physique et Chimie Marines, Station Marine de Villefranche-sur-Mer, 06230 Villefranche-sur-Mer, France

Abstract

Spectral measurements of downwelling and upwelling daylight were made in waters different with respect to turbidity and pigment content and from these data the spectral values of the reflectance ratio just below the sea surface, $R(\lambda)$, were calculated. The experimental results are interpreted by comparison with the theoretical $R(\lambda)$ values computed from the absorption and back-scattering coefficients. The importance of molecular scattering in the light back-scattering process is emphasized. The $R(\lambda)$ values observed for blue waters are in full agreement with computed values in which new and realistic values of the absorption coefficient for pure water are used and presented. For the various green waters, the chlorophyll concentrations and the scattering coefficients, as measured, are used in computations which account for the observed $R(\lambda)$ values. The inverse process, i.e. to infer the content of the water from $R(\lambda)$ measurements at selected wavelengths, is discussed in view of remote sensing applications.

The qualitative and quantitative analysis of dissolved and particulate matter from remote sensing values of the color of the ocean presents two problems. The first is the extraction of significant information from the signal received by a remote optical sensor. This involves an evaluation of the effects of reflection at the air–sea interface and of atmospheric attenuation and scattering that modify the upwelling radiant flux as it is just below the water surface. The second is the interpretation of the spectral composition of this flux in relation to the water's optical properties, which in turn are subordinate to the content of dissolved and particulate matter.

Only the second problem is examined here. Several studies have been made of the spectral analysis of downwelling irradiance just above the surface, $E_d(\lambda)$, and of upwelling irradiance just below the surface, $E_u(\lambda)$ (Morel 1973*a*; Morel and Caloumenos 1973; Morel and Prieur 1976*a*). These data were used to calculate spectral values for the reflectance ratio $R(\lambda)$ for "zero" depth by

$$R(\lambda) = E_u(\lambda)/E_d(\lambda)$$

(Morel and Prieur 1975). The corresponding graphs are shown in Fig. 1. The waters studied varied from the desert blue of the Sargasso Sea to those rich in phytoplankton and detrital particles, such as those encountered off the NW African coast in the productive upwelling areas.

The reflectance ratio, R, is particularly dependent on the inherent optical properties: the absorption coefficient (a), and the back-scattering coefficient (b_b). Their relationship can be expressed in the general form

$$R = F_{L\beta}(b_b/a).$$

The subscripts L and β emphasize that the function F is dependent on the radiance distribution and on the volume scattering function, $\beta(\theta)$, of the water. From the approximate theory of radiative transfer (the so-called two streams or Schuster's method) the preceding relationship can be formulated. Similar expressions were proposed by Gamburtsev in 1924 (*cited in* Kozlyaninov 1972) and by Duntley (1942) and Duntley et al. (1974) and involve the ratio of the diffuse back-scattering coefficient, b_b^*, to the diffuse absorption coefficient, a^*. With the hypotheses assumed by these workers, this ratio actually has the same value as the ratio $b_b : a$, where b_b and a are the usual coefficients defined for a collimated beam. In the sea $b_b : a \ll 1$, thus

[1] This work was supported in part by the Centre National de la Recherche Scientifique (RCP 247 & ERA 278) and in part by the Centre National d'Exploitation des Océans (under contract 75/1274).

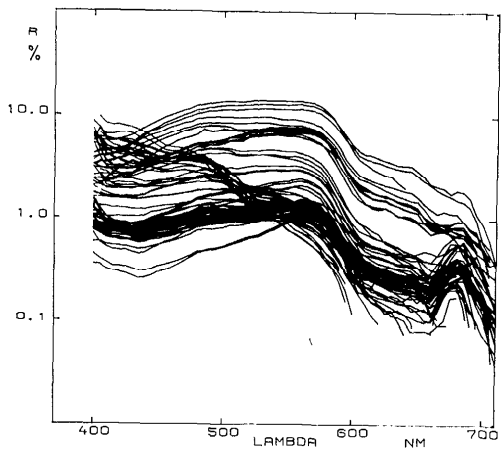

Fig. 1. Reflectance ratio $R(\lambda)$, expressed in percent, plotted with logarithmic scale vs. wavelength λ in nm, for 81 experiments in various waters. Same units and scales also used in Figs. 4, 5, 6, 7, and 11.

allowing the Gamburtsev-Duntley expressions to be transformed into

$$R = \tfrac{1}{2}(b_b : a)/(1 + b_b : a),$$

as mentioned by Kozlyaninov and Pelevin (1965).

Analyzing their numerical results obtained by a Monte-Carlo simulation of radiative transfer, Gordon et al. (1975) derived, by least-squares, analytical expressions for R having the form

$$R(\tau) = \sum_{n=0}^{n=3} r_n(\tau) x^n,$$

where x is $(b_b : a)(1 + b_b : a)^{-1}$, and τ is the optical depth. They tabulated the expansion coefficients $r_n(\tau)$ for diverse cases. At the depth $\tau = 0$, if the constant term $r_o(0)$ is neglected as very small and meaningless from a physical viewpoint, and if only the first term is kept, then $R = Cx$, with $C = 0.3244$ for the case where the sun is at its zenith and $C = 0.3687$ for a uniform sky.

Calculations of R using the successive order scattering method lead to the expression (Prieur and Morel 1975; Prieur 1976)

$$R = 0.33(b_b : a)(1 + \Delta),$$

where the corrective term Δ depends on the radiance distribution and, above all, on the volume scattering function. Even in considering the extreme cases, Δ, positive or negative, never exceeds 5%. Thus, for the calculations below, it will suffice to adopt the simple expression

$$R = 0.33(b_b : a). \tag{1}$$

Furthermore, if emphasis is placed on the spectral behavior of R rather than on its absolute values, the omission of Δ is of little importance, for it is only slightly variable throughout the part of the spectrum considered.

In order to interpret the experimental results of $R(\lambda)$ or to predict and calculate its spectral variations, we must first study the possible variations of the two terms b_b and a. The variations of b_b, the back-scattering coefficient, are discussed below in cases ranging from clear to turbid waters. When discussing a, we are led to examination of the case of bluc waters, where absorption is near its minimum, separate from that of other cases of various blue-green and green waters where different factors increase absorption. Therefore, we divide our presentation into two parts, one for each of these cases.

The back-scattering coefficient and its spectral dependence

From here on, to avoid confusion with other subscripts, the back-scattering coefficient will be noted b', instead of b_b as conventionally written. The subscripts w and p stand for molecular and particle scattering. The total scattering coefficient, b, is expressed as the sum $b = b_w + b_p$, and η is defined as the ratio

$$\eta = b_w : b. \tag{2}$$

Similarly, the back-scattering coefficient is expressed as $b' = b'_w + b'_p$. Also $\eta' = b'_w : b'$.

For molecular scattering $b'_w : b_w = \tfrac{1}{2}$. Thus b' can be written

$$b' = (\eta b/2) + (1 - \eta) b r_p, \tag{3}$$

where $r_p = b'_p : b_p$, and

$$\eta' = \eta/[\eta + 2(1 - \eta) r_p]. \tag{4}$$

The ratio r_p is of the order of a few percent or less. The mean volume scattering function for marine particles as previously proposed (Morel 1973*b*), leads to the value 1.2% for r_p.

While molecular scattering is a minor and often negligible factor when the total scattering is considered, the situation is quite different if back-scattering is considered by itself. Thus, with $r_p = 0.01$, η' is 0.83 when $\eta = 0.10$; these values describe very clear water ($b = 0.029$ m^{-1} at $\lambda = 500$ nm). For rather turbid oceanic waters, when for example $\eta = 0.01$ (i.e. when $b_{500} = 0.29$ m^{-1}), the ratio η' is still as high as 0.33. With molecular scattering in most cases playing an important role in back-scattering, and at the same time having high selectivity, it follows that η' and b' may vary greatly with wavelength. The wavelength dependence of molecular scattering can be expressed in terms of a power law, the most suitable exponent, n_w, being –4.3 (Morel 1974). A similar law, with the exponent n_p will be used for particle scattering. It may be recalled that n_p has the theoretical value (3-m) for a polydisperse system of particles, when the distribution is not truncated and follows a Junge law with the exponent –m (Morel 1973*b*). This law, with a value of m around 4, in most cases describes the actual distributions.

For two wavelengths λ_o and λ, b' can be written

$$b'(\lambda_o) = b'_w(\lambda_o) + b'_p(\lambda_o),$$

and

$$b'(\lambda) = b'_w(\lambda_o)\Lambda^{n_w} + b'_p(\lambda_o)\Lambda^{n_p},$$

where $\Lambda = \lambda : \lambda_o$.

Also

$$b'(\lambda) = b'(\lambda_o)\eta'_o\Lambda^{n_w} + (1-\eta'_o)\Lambda^{n_p}, \quad (5)$$

where $\eta'_o = b'_w(\lambda_o) : b'(\lambda_o)$. When the back-scattering coefficient $b'(\lambda_o)$ (and consequently η'_o) is known for a given wavelength, the spectral values of $b'(\lambda)$ can be computed using Eq. 5. To illustrate the possible variation of b', the ratio $b'_{380} : b'_{700}$ has been formed and plotted versus η'_o in the upper part of Fig. 2, where two

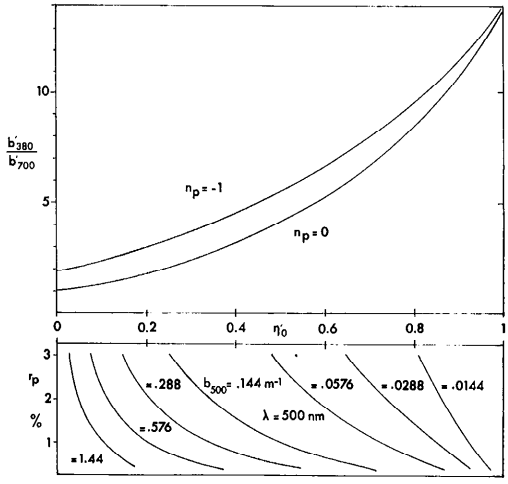

Fig. 2. Upper—ratio of back-scattering at $\lambda = 380$ and 700 nm plotted vs. parameter η'_o. Lower—variations of η'_o with parameter r_p for selected values of b, scattering coefficient at $\lambda = 500$ nm (in m^{-1}).

curves corresponding to a nonselective ($n_p = 0$) and a slightly selective ($n_p = -1$) particle scattering are given.

The variation of η'_o depicts the variation of the water's turbidity. By using Eq. 4, with a given value for r_p, it is possible to derive for each value of η'_o the corresponding value of η_o. Then, by fixing the value of the wavelength (for example $\lambda_o = 500$ nm, where $b_w = 0.00288$ m^{-1}) for each value of η_o, the corresponding value of b can be calculated by Eq. 2. The lower part of Fig. 2 shows the correspondence between η'_o and b_{500} when the parameter r_p varies between reasonable limits.

For optically pure water (when $\eta'_o \equiv 1$), the ratio between the back-scattering coefficients $b'_{380} : b'_{700}$ is obviously equal to $(700:380)^{4.3}$ (i.e. 13.8). Conversely, for very turbid waters (when $\eta'_o \to 0$), the above ratio tends toward 1 or toward 700:380 (i.e. 1.84) according to the value adopted for n_p.

It is important to point out that for usual oceanic surface waters (b up to 0.5 m^{-1}), not only for the clearest (b near 0.03 m^{-1}), the wavelength dependence of b', as illustrated by this ratio, must always be taken into consideration.

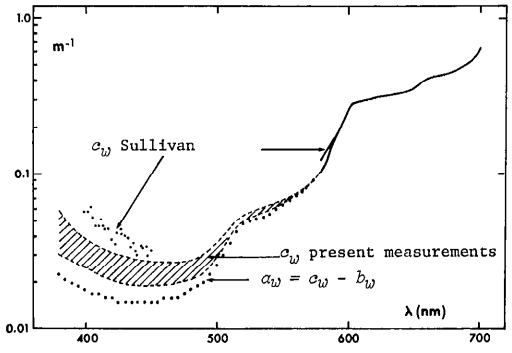

Fig. 3. Attenuation, $c_w(\lambda)$, and absorption coefficient, $a_w(\lambda)$, expressed in m^{-1}, for pure water.

Part 1: Blue waters

Deep blue is the characteristic color of very pure natural water, but suspended particles are present even in the purest of these. It is probable that absorption is always somewhat higher for natural waters than for chemically pure water, or pure seawater (meaning without any trace of dissolved organic substances). However the absorption values for the limiting case of pure water must be examined first.

Absorption coefficient for pure water—Of the attenuation, absorption, and scattering coefficients, c_w, a_w, and b_w, the last is the best known for optically pure water or optically pure seawater (Morel 1974). By subtraction, a_w could be obtained if the c_w values were well known. However, it is difficult to choose among the published values for c (Jerlov 1968). The values presented by Clarke and James (1939) are often used, but these data were obtained at large intervals of wavelength and are too irregular to permit meaningful interpolation, especially in the 400–580-nm spectral region. The results of Sullivan (1963) are probably the most reliable but unfortunately do not cover the 450–580-nm band.

We have made measurements using a Beckman DU spectrophotometer, modified to allow use of 110-cm cells by adding a field stop and an achromatic objective lens to provide a collimated beam along the 110-cm path. At the exit of the cell, two field stops prevent most of the scattered light surrounding the beam from reaching the receiver. The measurements were conducted from 380–700 nm by comparison with an empty reference cell. The corrections for reflection were calculated from the Fresnel formula. The water filling the cell was purified according to the following procedure. Distilled water was evaporated without boiling and then condensed on a cooled quartz surface from which it flowed directly into the sample cell; this process was repeated several times to purify the water and simultaneously to clean the cell. Despite all efforts, and because of the optical imperfections of this arrangement, our absolute values for c remain in question.

The calibration factor, though inaccurately known, may be thought of as constant throughout the spectrum, and the c values obtained in the 380–700-nm band may be adjusted to coincide with Sullivan's values in the 600–800-nm spectral band.

With this normalization, all the $c(\lambda)$ curves (only the two extremes are drawn) fall inside the shaded area shown in Fig. 3, and it appears that these curves are below Sullivan's values in the range 400–450 nm. The uncertainties in the measurements in the region of the greatest transmission cause the divergence of the results at 500–380 nm. The lowest values obtained are associated with a less marked increase between 420 and 380 nm. This seems to be a sensitive criterion for success in purifying the water, and we therefore selected the lowest values of $c_w(\lambda)$ to obtain $a_w(\lambda)$ (Table 1). The $b_w(\lambda)$ values subtracted from $c_w(\lambda)$ are those of optically pure water (Morel 1974). There are two main points of interest: one is the c (and a) minimum between 430 and 470 nm, which is almost flat; the other is the slight but notable increase in absorption between 500 and 520 nm with a slope structure similar to the well known discontinuity arising around 600 nm. These results, particularly the low values around the absorption minimum, are confirmed by values for clear natural waters independently obtained through an indirect method (*see below*).

Table 1. Attenuation (c_w), scattering (b_w), and absorption (a_w) coefficients for optically (and chemically) pure water.

λ (nm)	c_w	b_w	a_w	λ (nm)	c_w	b_w	a_w	λ (nm)	$c_w \sim a_w$	b_w
		(m^{-1})				(m^{-1})				(m^{-1})
380	0.030	0.0073	0.023	490	0.022	0.0024	0.020	600	0.245	0.00101
390	0.027	0.0066	0.020	500	0.028	0.0022	0.026	610	0.290	0.00094
400	0.024	0.0058	0.018	510	0.038	0.0020	0.036	620	0.310	0.00088
410	0.022	0.0052	0.017	520	0.050	0.0018	0.048	630	0.320	0.00082
420	0.021	0.0047	0.016	530	0.053	0.0017	0.051	640	0.330	0.00076
430	0.019	0.0043	0.015	540	0.058	0.0016	0.056	650	0.350	0.00071
440	0.019	0.0039	0.015	550	0.066	0.0015	0.064	660	0.410	0.00067
450	0.018	0.0035	0.015	560	0.072	0.0013	0.071	670	0.450	0.00063
460	0.019	0.0032	0.016	570	0.081	0.0013	0.080	680	0.450	0.00059
470	0.019	0.0029	0.016	580	0.109	0.0012	0.108	690	0.500	0.00055
480	0.021	0.0027	0.018	590	0.158	0.0011	0.157	700	0.650	0.00052

Calculation of the reflectance ratio R(λ)—We carried out calculations in 5-nm increments using Eq. 1 and the absorption coefficients for pure water (Table 1). The scattering was considered as variable, starting from the ideal limiting case where it is due only to molecular scattering. Each computed case is defined by a pair of values given to the parameters r_p and X, where $X = b_p : b_w$ at the wavelength $\lambda_o = 500$ nm, and r_p is assumed constant throughout the spectrum. From a physical point of view one parameter would suffice to define each case, for instance the product r_pX, since only the magnitude of the back-scattering is of importance.

The constant $b_{w,500}$, equal to 0.00288 m^{-1} at $\lambda_o = 500$ nm, is introduced in the calculation and thus $b_{500} = b_{w,500}(1 + X)$ and $\eta = 1/1 + X$. Note that the $b_w(\lambda)$ values that were subtracted from $c_w(\lambda)$ to obtain $a_w(\lambda)$ are those for optically and chemically pure water. The $b_w(\lambda)$ values used here pertain to optically pure seawater, which are about 30% higher (Morel 1974).

We can now calculate b'_{500} and η'_{500} by Eq. 3 and 4. The spectral values of $b'(\lambda)$ are obtained through Eq. 5 and are combined with the absorption values $a_w(\lambda)$, using Eq. 1, in the range 380–700 nm.

Figure 4 shows the spectral reflectance ratio computed for five cases with an increasing back-scattering as indicated in the inset. The lowest curve (T1) represents the limiting case of optically pure water. In this case, the spectral variation of $R(\lambda)$ has its greatest amplitude because the back-scattering coefficient varies according to the $\lambda^{-4.3}$ law. The theoretical results obtained by Maul and Gordon (1973) differ from those presented here mainly because their values for water absorption and scattering are not the same as those we used. Maul and Gordon (1975) later adopted other values which still lead to R values markedly lower than those given here, by about 35–45% in the reference case of pure water. To make a comparison we have applied a factor of 0.54 to transform the R values below the surface into R values above the surface, since Maul and Gordon's computations concern the latter. This factor is due to the refraction effect at the sea–air interface, assumed to be perfectly flat (Austin 1974). For the other cases (T2–T5), the absorption remains that of pure water, but particles are present in increasing amounts. Two effects arise simultaneously: all the $R(\lambda)$ values increase with back-scattering and the spectral distribution is changed, leading to a flattening out of the curve with a shift of the maximum toward longer wavelengths. These spectral changes are due to reduction of back-scattering selectivity and they are of less importance, for a given concentration of particles, if the particle scattering is slightly selective (dotted curves with $n_p = -1$).

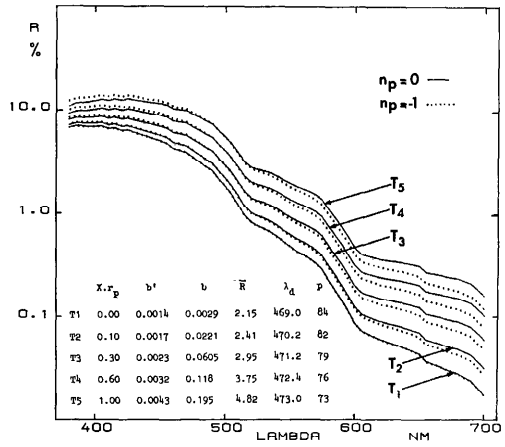

Fig. 4. Theoretical reflectance ratio computed with $a_w(\lambda)$, absorption by pure water, and for increasing back-scattering (from T1–T5). Inset: back-scattering and scattering coefficients b' and b are given for $\lambda = 500$ nm and with assumption $r_p = 1.5\%$. $\overline{R}$ is reflectance ratio for whole spectrum, expressed in percent.

Chromaticity coordinates for each curve computed in reference to CIE system. From these, dominant wavelengths (λ_d) and excitation purities (p, %) have been deduced. Listed values correspond to dotted curves ($n_p = -1$).

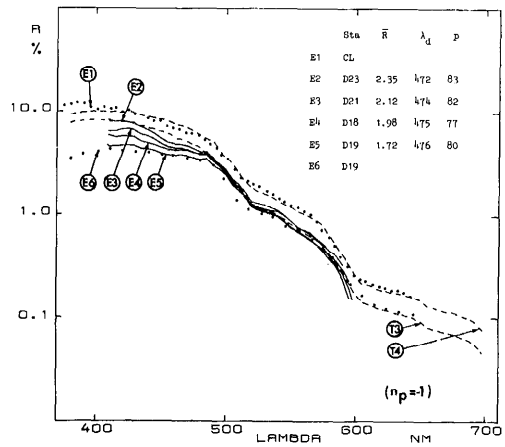

Fig. 5. Theoretical dashed curves T3 and T4 (with $n = -1$) taken from Fig. 4. Experimental dotted curve E1 concerns Crater Lake (Oregon); E2–E6 concern Sargasso Sea and these experiments were carried out during Discoverer cruise (stations D23, D21, D18, and D19). E6 deduced from Smith's (1973) values obtained at a depth of 5 m and is close to that corresponding to zero depth (E5) at same station. $\overline{R}$ is computed within interval where spectral data are available and significant. λ_d and p have same meaning as in Fig. 4.

Both these effects are equally described by the variations of the quantities listed in the inset. From case 1 to case 5, the mean reflectance ratio $\overline{R}$ (obtained by integration of $R(\lambda)$ between 380 and 700 nm) increases twofold. The dominant wavelength, λ_d, increases while excitation purity p decreases. The human eye would perceive a slight shift from deep blue to blue-green, and a brighter but less pure color, as the particles in suspension increase.

Comparison with experimental results—Results from Crater Lake (Tyler and Smith 1970) and the Sargasso Sea (Morel 1973*a*; Morel and Prieur 1975) are taken as representative of blue waters. They are shown as the curves in Fig. 5 and the related information is given in the legend.

The spectral reflectance for station 23 in the Sargasso Sea (E2) agrees well with the theoretical curve T3 (with $n_p = -1$). At this station the water was the clearest observed, and the absorption coefficients, $a(\lambda)$, computed for the upper layer (Morel and Prieur 1975) approach those of Table 1 (*see also Figs. 8 and 9*).

The experimental R values for stations 21, 18, and, notably, 19 are lower than the theoretical ones below 480 nm. A small amount of phytoplankton (the chlorophyll a + pheophytin a concentration is 0.04 mg m^{-3} at station 19: Baird 1973) probably associated with a slight amount of yellow substance, explains the increase in absorption and consequently the decrease of R in the blue-violet part of the spectrum. For these stations the attenuation coefficient c was about the same, ca. 0.08 m^{-1} for $\lambda = 491$ nm (Austin 1973), leading to a value for b of around 0.06 m^{-1}, which coincides with the value used in the computation. Hence the value given to r_p, i.e. 1.5%, seems reasonable. Moreover, the back-scattering coefficients at $\lambda = 500$ nm have been computed from the downwelling and upwelling irradiance data collected at these stations (Morel and Prieur 1975). The values obtained lie between 0.0022 and

0.0029 m^{-1} and are in agreement with that introduced in the calculation of T3 (0.0023 m^{-1}). The spectral reflectance curve for Crater Lake (E1) fits the theoretical curve T4 (with $n_p = -1$). This confirms the purity of the lake water relative to absorption, but the particle back-scattering is twice that for the Sargasso Sea. This is caused either by a higher particle concentration or by a higher back-scattering efficiency. The lack of scattering data prevents distinguishing between these possibilities.

In conclusion, it appears that a satisfactory theoretical explanation exists for spectral R values and for color in the case of these very clear waters.

Part 2: Various green waters

In these variously productive and turbid waters the presence of dissolved and suspended matter increases both absorption and scattering. When the back-scattering increases, R values increase more or less uniformly throughout the spectrum. Conversely, the rise in absorption diminishes R, especially in the spectral bands corresponding to the specific absorption of the various substances present. Thus the shape of the spectral reflectance curve may be diversely modified.

Among the curves corresponding to green waters shown in Fig. 1, two extreme cases can be identified and separated. Case 1 is that of a concentration of phytoplankton high compared to that of other particles. The pigments (chlorophylls, carotenoids) play a major role in actual absorption. In contrast, the inorganic particles are dominant in case 2, and pigment absorption is of comparatively minor importance. In both cases dissolved yellow substance is present in variable amounts and also contributes to total absorption. An ideal case 1 would be a pure culture of phytoplankton and an ideal case 2 a suspension of nonliving material with a zero concentration of pigments. Obviously, these ideal situations are not encountered in nature, and the most representative examples of cases 1 and 2 have been selected on the basis of high or low values of the ratio of pigment concentration : scattering coefficient. It must be kept in mind that intermediate situations with intermediate values of this ratio are in fact more common.

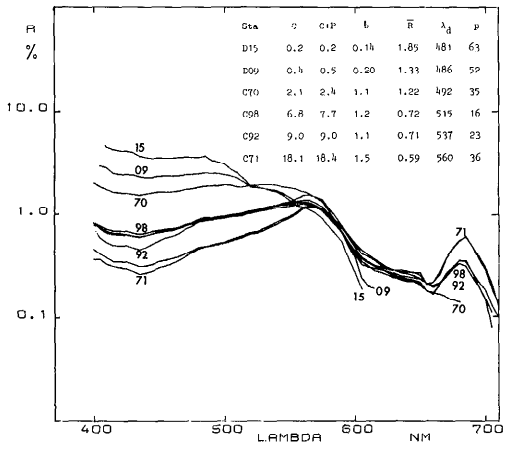

Fig. 6. Experimental $R(\lambda)$ curves for different stations listed in inset: D stations—Discoverer cruise; C stations—CINECA 5-Charcot cruise. C and C+P—chlorophyll *a* and the chlorophyll *a* + pheophytin *a* concentration in mg m^{-3}; *b*—scattering coefficient at 550 nm. Curves illustrate case 1 (*see text*).

Case 1—Figure 6 corresponds to situations where the chlorophyll concentration is high relative to the scattering coefficient (*see inset*). As the pigment concentration increases several changes occur—

1. The R values in the blue-violet region decrease progressively and a minimum is formed around 440 nm, which corresponds to the maximum absorption of chlorophyll. The maxima shift toward 565–570 nm, which is the wavelength where simultaneously the absorption due to pigments is at its minimum and the absorption due to the water itself rapidly increases. The irregularity near 480 nm may be attributed to carotenoids.

2. The second maximum of absorption by chlorophyll *a* in vivo creates an R minimum near 665 nm. This minimum is only slightly marked because the increase in absorption due to the presence of chlorophyll remains weak compared with the absorption due to the water itself.

3. At 685 nm a second maximum ap-

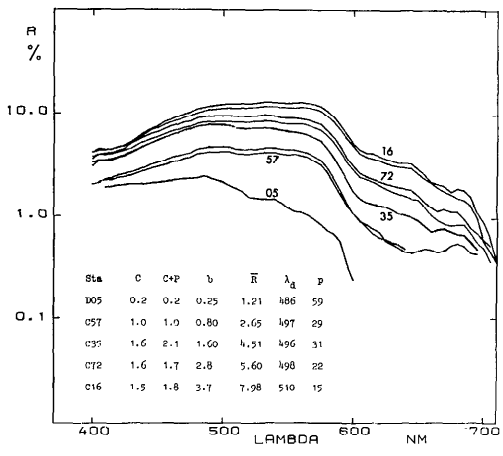

Fig. 7. Experimental $R(\lambda)$ curves illustrating case 2 (*see text*). Symbols same as for Fig. 6.

pears. This feature is also noticeable in the results of experiments carried out in the San Vincente Reservoir by Tyler and Smith (1970). Latimer (1963) reported that scattering by pigmented particles such as microalgae is spectrally affected in the vicinity of the absorption bands, and that the spectral scattering curves resemble an anomalous dispersion curve. The enhancement of scattering and of back-scattering on the long wavelength side of the absorption peak could explain the existence of the R maximum at 685 nm. Gordon (1974), considering the data of Tyler and Smith, favored such an interpretation. Another phenomenon must be taken into consideration, which probably combines its effect with the preceding one. The fluorescence emission spectrum of chlorophyll *a* in vivo peaks at 685 nm, and this emission would be detectable in the upwelling light field because of its low level while it remains undetected in the downwelling flux. The influence of this emission can be confirmed by the different behaviors of K_d and K_u, the attenuation coefficients for downwelling and upwelling irradiances. The diffuse attenuation coefficient K is defined by $K = -d(\ln E)/dz$, where E is irradiance at depth z. If E is the down- or upwelling irradiance, the corresponding coefficient is denoted as K_d or K_u. K_d exhibits a maximum near 660–670 nm whereas for K_u this maximum is partially truncated and, moreover, a minimum appears at 685 nm (Morel and Prieur 1975).

4. For the examples shown in Fig. 6, the R values in the 560–640-nm band are roughly the same, whereas b varies approximately in the ratio 10:1 between the extreme cases. This implies that the absorption increase, in the ratio 4:1 (*see Fig.* 8), is nearly compensated by the back-scattering increase, which appears smaller than the total scattering increase. The ratio 4:1 can be obtained with Eq. 3 if r_p is considered as variable between 1.5% (for station D15) and 0.5% (station C71).

5. The mean reflectance ratio (calculated for the visible spectrum) becomes very low when the amount of phytoplankton increases. At the same time, the color changes from blue-green to dark green-brown, as demonstrated by the values of λ_d and p.

Case 2—Figure 7 illustrates waters relatively higher in inorganic particles than in phytoplankton. As the turbidity increases the following modifications appear—

1. The R values are generally higher than for case 1 throughout the spectrum and of a different shape. There is no longer, as in case 1, a minimum at 440 nm. On the contrary, the curves become convex between 400 and 560 nm. The maximum is flatter than in case 1, but located at the same wavelength, 560 nm.

2. The increase in back-scattering is not compensated by a proportional increase in absorption, since R values become higher as turbidity increases. This is opposite of what was observed in case 1, particularly for wavelengths above 550 nm.

3. As a result of the flat shape of the R curves, the dominant wavelength does not shift beyond 510 nm. These waters are blue-green or green with a bright and milky appearance due to the combined effects of high $\bar{R}$ values and of low purity values.

Interpreting the spectral reflectance behaviors requires a special examination of spectral absorption coefficients in the case of these various green waters.

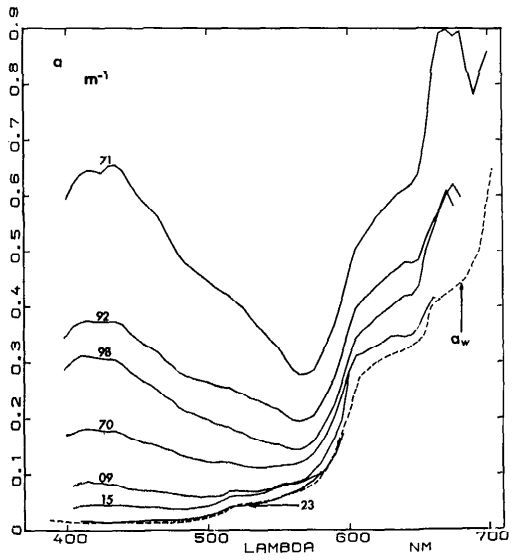

Fig. 8. Spectral values of absorption coefficient, expressed in m^{-1}, for same stations as in Fig. 6. In addition, values for station Discoverer 23 (Sargasso Sea) and for pure water (labeled a_w) are plotted.

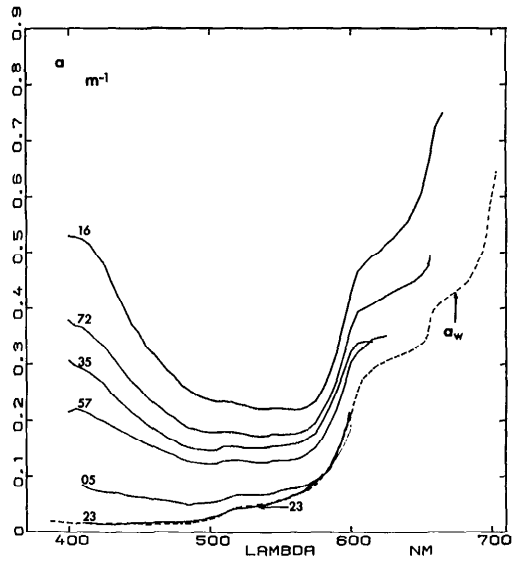

Fig. 9. Spectral values of absorption coefficient, expressed in m^{-1}, for same stations as in Fig. 7.

Spectral values of the absorption coefficient—At the stations where $R(\lambda)$ was determined, values of the downwelling irradiance, $E_d(\lambda)$, were also recorded for different depths; thus the diffuse attenuation coefficient, $K_d(\lambda)$, can be obtained. With these results and using expressions similar to those established by Preisendorfer (1961), we computed the absorption coefficients $a(\lambda)$ for the surface layer (Morel and Prieur 1975). Figures 8 and 9 show the $a(\lambda)$ curves for the surface layer at the same stations as in Figs. 6 and 7.

The $a(\lambda)$ curves, which would be called V-shaped and U-shaped, are associated with the concave and convex $R(\lambda)$ curves. In case 1 the V-shape and the peaks at 440 and 670 nm result mainly from carotenoid and chlorophyll absorption. In these examples, the pheophytin concentration is low compared to the chlorophyll concentration, and its influence on absorption can be thought of as remaining weak. In case 2 there is no peak, but a regular increase in absorption toward the shorter wavelength, and the minimum between 500 and 570 nm is broad and flat. Suspended nonliving material is assumed to be the main cause of this absorption. However, the dissolved humic substances ("yellow substance") also contributes to the absorption, at least in the blue-violet part of the spectrum. This is also true for case 1, but the role of humic substances cannot be estimated on the basis of these experiments alone. However in some stations during the CINECA-Charcot 5 cruise, the absorption by dissolved matter was measured in the range 380–550 nm, allowing for a more complete description (Prieur 1976; Morel and Prieur 1976*b*).

From pairs of stations where the scattering coefficients, b, are about the same, but where the pigment concentrations differ, it is possible to subtract one $a(\lambda)$ curve from the other and thus obtain $a(\lambda)$ values attributable to the pigments alone. These values can be normalized to unit pigment concentration (actually 1 mg m^{-3} of Chl a). In the same manner, an absorption spectrum for the nonliving material can be obtained from pairs of stations where pigment contents are similar but scattering coefficients differ. This spectrum can be standardized also to a unit particle concen-

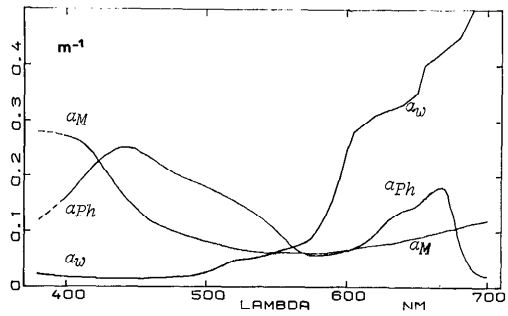

Fig. 10. Spectral values, expressed in m^{-1}, of absorption coefficients: a_w—for pure water; a_{Ph}—for natural phytoplankton pigments at concentration corresponding to Chl *a* concentration of 10 mg m^{-3}; a_M—for suspended and dissolved materials, apart from algae, at concentration corresponding to scattering coefficient of 2 m^{-1} (at 550 nm).

tration, arbitrarily defined as that which corresponds to the b value equal to 1 m^{-1} at 550 nm.

Several pairs of stations were used for such calculations and the results, which have been averaged, are shown in Fig. 10. The $a_{Ph}(\lambda)$ curve represents natural phytoplankton absorption. The $a_M(\lambda)$ is representative of absorption due to all materials, suspended and dissolved, other than the algal cells. This is only a rough approach. With this procedure the light-absorbing factors cannot be classified into more than two classes, and, for example, the specific influence of pheopigments or of the humic substances cannot be isolated. On the other hand, the a_{Ph} specific spectrum depicts a mean situation for the pigment composition of the algal cells. In the same manner, but more questionably, a_M represents a mean proportion between dissolved and particulate detrital matter.

The a_{Ph} spectrum is similar to that obtained by Lorenzen (1972) for a natural population of algae and also to some of those obtained by Duntley et al. (1974) for different algal cultures. Moreover, the a_{Ph} values agree well with Duntley's values given also for unit chlorophyll *a* concentration. But this a_{Ph} spectrum differs both qualitatively and quantitatively from the spectrum obtained by Yentsch (1960). In particular, the residual absorption between 560 and 600 nm is much higher than that reported by Yentsch.

Comparison between experimental and computed R(λ) curves—It follows from Eq. 1 that if $R(\lambda)$ and $a(\lambda)$, the latter deduced from $K_d(\lambda)$, are known, the back-scattering coefficient can be computed. This has been done (Morel and Prieur 1975) and the results were discussed by Prieur (1976).

Another aspect of the problem originates through use of remote sensing. It is assumed that, after correction for atmospheric deterioration and illumination change, quantities proportional to $R(\lambda)$ are obtained and form the only available information about an unknown marine area. To find out if such values can provide an estimation of pigment concentration and turbidity, we can carry out a trial using the present R measurements for which the above mentioned parameters are known. This trial will consist of properly reconstructing the experimental $R(\lambda)$ curves by computations using the sea truth values. If satisfactory reconstruction is obtained, it should be possible in turn to solve the inverse problem, i.e. to interpret $R(\lambda)$ data deduced from remote measurements.

The computation is made as follows. The specific spectra previously given are used to calculate the absorption coefficients by

$$a(\lambda) = a_w(\lambda) + [C + P]a_{Ph}(\lambda) + ba_M(\lambda), \quad (6)$$

where [C + P] is the concentration of chlorophyll *a* and pheophytin *a* expressed in mg m^{-3} and b is the scattering coefficient. The b value determines unequivocally the value of the X parameter. The r_p parameter ($r_p = b_b : b$) is adjusted in such a way that the computed and experimental R values are close in the vicinity of 500 nm.

Some selected experimental curves are shown in Fig. 11 with the corresponding computed curves. Cases 1 and 2 are represented by the typical stations C98 and C16; the others stand for intermediate situations. Agreement is always obtained with r_p values around 0.5% for the stations belonging to or approaching case 1. The detrital par-

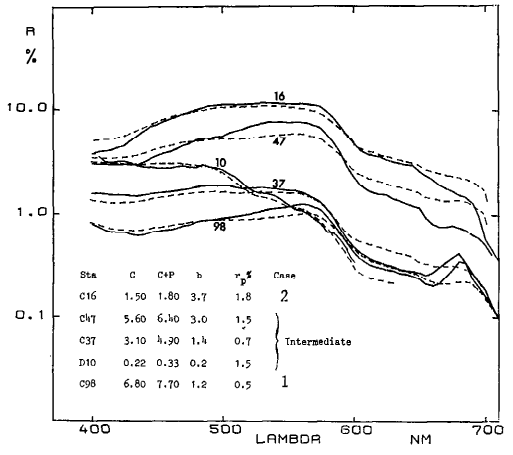

Fig. 11. Solid curves—experimental $R(\lambda)$ curves for stations listed in inset (D for Discoverer, C for Charcot cruises). Dashed curves—theoretical $R(\lambda)$ curves (same stations) computed with measured scattering coefficient b (at 550 nm, in m^{-1}) and pigment concentration (chlorophyll a + pheophytin a, column C+P, in mg m^{-3}). Column r_p gives adjusted values of this parameter to obtain best agreement in each case between computed and actual $R(\lambda)$ curves.

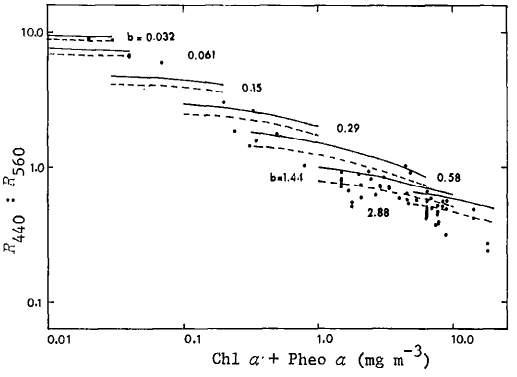

Fig. 12. Ratio of reflectance ratios at 440 and 560 nm, plotted vs. pigment concentration (Chl a + Pheo a, in mg m^{-3}). Both scales logarithmic. Dots—experimental values; curves—computed variations of same ratio ($n_p = -1$: solid lines; $n_p = 0$: dashed lines).

ticles in case 2 are probably more refringent; consequently the best r_p values appear to be about 1.5%, as was also true for the blue waters. For all cases, agreement between calculation and experiment is better if particle scattering is taken to be slightly selective ($n_p = -1$).

This agreement can be regarded as satisfactory in the 400–600-nm region since the concave and convex shapes, or the flat shape in the intermediate situation, can be neatly reproduced. This is not the case if the absorption coefficients for plant pigments given by Yentsch (1960) are used in the computations. Beyond 600 nm the computed curves are often below the experimental curves when they are made to coincide in the 400–500-nm interval, as can be done by adjusting r_p. This discrepancy could be due to a reduction of back-scattering by the pigmented particles precisely in the spectral range where they absorb. This possibility cannot be ascertained because the experimental $R(\lambda)$ values in the red part of the spectrum may be underestimated. Note that $E_u(\lambda)$ is measured below the surface at a depth which in practice cannot be rigorously "zero"; the values determined are thus lower than they would have been at exactly zero depth. The more pronounced this effect is, the higher the absorption, as is the case mainly in the red. The underestimated R values theoretically could be corrected (*see* Morel and Prieur 1975), but such a correction is arbitrary because the true measurement depth, variable between 0.2 and 1 m, is unknown. Obviously the computation cannot account for the occurrence of a peak at 685 nm, whether the origin of the peak is a change in scattering, a fluorescence emission, or both.

Discussion and conclusion

If we go back to the initial problem of interpreting $R(\lambda)$ data deduced from remote measurements, the quality of the reconstruction, at least in the spectral region 400–600 nm, does permit solution. While the reconstruction is done with two variable terms in absorption, these two terms could be deduced conversely from an $R(\lambda)$ spectrum. However, this conclusion rests on a comparison of absolute $R(\lambda)$ values. As is shown below, other problems arise if only relative $R(\lambda)$ values are available.

In remote-sensing applications it seems reasonable to use the ratios of the signals obtained in different wavelength bands but with the same geometrical conditions regarding the tilt angle and the field of view. For instance Clarke et al. (1970) and Clarke and Ewing (1974) proposed use of a "color ratio," defined as the ratio of the signals received at 460 and 540 nm. Other pairs of wavelengths have been suggested (443 and 525 nm: Arvesen et al. 1973). From our results, the ratio $\rho = R_{440}:R_{560}$ has been formed and Fig. 12 shows it plotted versus the pigment [Chl a + Pheo a] concentration measured at the same locations. The wavelengths 440 and 560 nm were chosen as more precisely those of the absorption maximum and minimum for the plant pigment (*see also Fig. 10*). The distribution of points in Fig. 12 showed a very rough linear relationship between the logarithms of the plotted quantities. The scattering of the dots implies that using ρ to infer pigment concentration leads to an ambiguous answer; for instance, the same value of ρ can be observed while pigment concentration varies in a ratio of 10:1.

The variations in ρ are explainable, according to Eq. 1, by the combined influences of $a_{560}:a_{440}$ and $b_{b,440}:b_{b,560}$. The first ratio decreases when pigment concentration increases, but the presence of detrital material has the same effect. The second ratio varies mainly because of the variable influence of molecular scattering (Eq. 5). It diminishes when particle scattering rises and in general enhances the variations of the first ratio. The values of ρ have been computed by means of Eq. 1, 5, and 6, and by using the specific absorptions a_{Ph} and a_M. For each pigment concentration range, realistic values have been given for b_{500}, the total scattering coefficient at $\lambda = 500$ nm. The other parameters are $r_p = 1.5\%$ and $n_p = -1$ or 0. The computed curves account for the spread of the experimental dots. The highly selective molecular scattering is responsible for the high values of ρ at low pigment concentrations. At high pigment concentrations the ambiguity pointed out above is fully understandable if one considers that the scattering value determines the ρ value as much as or more than the pigments do.

It is obvious that measurements at two wavelengths, obtained in relative units and used in the form of a ratio, produce only one number and thus cannot provide information about scattering and absorption and moreover cannot discriminate between different absorbing agents. It is useful to examine what can be expected from a multispectral method.

First, there appears to be no spectral band in which the influence of a single absorbing component can be completely isolated. If these components are classified into two categories, as done here, there is no spectral domain where the absorption by one is negligible compared to the absorption by the other. If we attempt to distinguish between more than two absorbing agents, such as different chlorophyll forms, pheopigments, or yellow substance, etc., the above conclusion remains valid according to the available results for their specific absorption spectra. The fact that, whatever the wavelength, several absorbers come into play does not prevent solution of the problem, at least from a theoretical point of view. Multispectral measurements in relative units at $N + 1$ wavelengths allow the inference of concentration of N absorbing compounds. The N absorption ratios, as $a(\lambda_i):a(\lambda_j)$, are introduced in a system of N linear equations. However to write this system, we need to know the specific absorption spectrum for each of the N desired components. Further efforts are required to develop such a catalogue of spectral signatures.

Another point must be emphasized relative to scattering. As has been shown, the role of molecular scattering in the light back-scattering process cannot be neglected in most cases. For this reason, as exemplified by Fig. 12, the value of a ratio such as ρ is partly determined by the ratio of the back-scattering coefficients, which generally differs from unity. Consequently, in the case of multispectral measurements at $N + 1$ wavelengths, N additional unknowns arise, i.e. the N ratios $b_b(\lambda_i):b_b(\lambda_j)$. These N unknowns can be reduced to one un-

known only if the spectral dependence of the particle scattering is assumed to obey a simple law, for instance a power law as used here. Nevertheless, even with only one additional unknown the system becomes undetermined. The indeterminancy is greater if such a simple selectivity law cannot be regarded as realistic, as is likely in the case of scattering by algal cells. If no rigorous solution is possible, iterative processes have to be applied in combination with empirical laws. Natural conditions impose limits which restrict plausible solutions. For instance, it is unlikely that high pigment concentrations will coexist with low scattering values. Such natural rules may improve and guide the iterative computations.

Finally, the relationship between the reflectance ratio and the absorption and back-scattering coefficients (Eq. 1), despite its approximate character, accounts for experimental results within a reasonable degree of accuracy. It would appear that attempts to refine this relationship at the price of tedious calculations of radiative transfer are less needed at present than is an increase in optical and oceanographic research aimed at better understanding the absorbing and scattering properties of the materials present in the sea.

References

ARVESEN, J. C., J. P. MILLARD, AND E. C. WEAVER. 1973. Remote sensing of chlorophyll and temperature in marine and fresh waters. Astronaut. Acta **18**: 229–239.

AUSTIN, R. W. 1973. Transmittance, scattering and ocean color, p. J1–J132. *In* SCOR Data Rep. Discoverer Expedition, v. 2. Scripps Inst. Oceanogr. Ref. 73-16.

———. 1974. The remote sensing of spectral radiance from below the ocean surface, p. 317–344. *In* N. G. Jerlov and E. Steemann Nielsen [eds.], Optical aspects of oceanography. Academic.

BAIRD, I. E. 1973. Chlorophyll concentration and phaeopigments, p. C1–C25. *In* SCOR Data Rep. Discoverer Expedition, v. 1. Scripps Inst. Oceanogr. Ref. 73-16.

CLARKE, G. L., AND G. C. EWING. 1974. Remote spectroscopy of the sea for biological production studies, p. 389–414. *In* N. G. Jerlov and E. Steemann Nielsen [eds.], Optical aspects of oceanography. Academic.

———, ———, AND C. J. LORENZEN. 1970. Spectra of back-scattered light from the sea obtained from aircraft as a measure of chlorophyll concentration. Science **167**: 1119–1121.

———, AND H. R. JAMES. 1939. Laboratory analysis of the selective absorption of light by sea water. J. Opt. Soc. Am. **29**: 43–55.

DUNTLEY, S. Q. 1942. Optical properties of diffusing materials. J. Opt. Soc. Am. **32**: 61–70.

———, W. H. WILSON, AND C. F. EDGERTON. 1974. Ocean color analysis, part 1. Scripps Inst. Oceanogr. Ref. 74-10.

GORDON, H. R. 1974. Spectral variation in volume scattering function at large angles in natural waters. J. Opt. Soc. Am. **64**: 773–775.

———, O. B. BROWN, AND M. M. JACOBS. 1975. Computed relationships between the inherent and apparent optical properties of a flat homogeneous ocean. Appl. Opt. **14**: 417–427.

JERLOV, N. G. 1968. Optical oceanography. Elsevier.

KOZLYANINOV, M. V. 1972. The basic relationships between the hydro-optical parameters, p. 5–24. *In* K. S. Shifrin [ed.], Optics of the ocean and the atmosphere [in Russian]. Nauka.

———, AND V. N. PELEVIN. 1965. On the application of a one-dimensional approximation in the investigation of the propagation of optical radiation in the sea [in Russian]. Tr. Inst. Okeanol. Akad. Nauk SSSR 77, p. 73–79. *Also* 1966. U.S. Dep. Comm., Jt. Publ. Res. Ser. Rep. **36**(816): 54–63.

LATIMER, P. 1963. Is selective scattering a universal phenomenon?, p. 213–225. *In* Studies on microalgae and photosynthetic bacteria. Jap. Soc. Plant Physiol. Univ. Tokyo.

LORENZEN, C. J. 1972. Extinction of light in the ocean by phytoplankton. J. Cons., Cons. Int. Explor. Mer **34**: 262–267.

MAUL, G. A., AND H. R. GORDON. 1973. Relationships between ERTS radiances and gradients across oceanic fronts, p. 1279–1308. *In* Proc. ERTS Symp. (3rd).

———, AND ———. 1975. On the use of the Earth Resources Technology Satellite in optical oceanography. Remote Sensing Environ. **4**: 95–128.

MOREL, A. 1973*a*. Measurements of spectral and total radiant flux, p. F1–F341. *In* SCOR Data Rep. Discoverer Expedition, v. 1. Scripps Inst. Oceanogr. Ref. 73-16.

———. 1973*b*. Diffusion de la lumière par les eaux de mer. Résultats expérimentaux et approche théorique, p. 31.1–31.76. *In* Optics of the sea. AGARD Lect. Ser. 61.

———. 1974. Optical properties of pure water and pure sea water, p. 1–24. *In* N. G. Jerlov

and E. Steemann Nielsen [eds.], Optical aspects of oceanography. Academic.

———, AND L. CALOUMENOS. 1973. Mesure d'éclairements sous-marins, flux de photons et analyse spectrale. Centre Rech. Oceanogr. Villefranche-sur-Mer Rapp. 11. 242 p.

———, AND L. PRIEUR. 1975. Analyse spectrale des coefficients d'atténuation diffuse, de réflexion diffuse, d'absorption et de retrodiffusion pour diverses régions marines. Centre Rech. Oceanogr. Villefranche-sur-Mer Rapp. 17. 157 p.

———, AND ———. 1976*a*. Irradiation journalière en surface et mesure des éclairements sous marins, p. 1–256. *In* Résultats de la campagne CINECA 5 (Groupe Médiprod), Sect. 1–1-10. Publ. CNEXO.

———, AND ———. 1976*b*. Analyse spectrale de l'absorption par les substances dissoutes (substances jaunes), p. 1–9. *In* Résultats de la campagne CINECA 5 (Groupe Médiprod), Sect. 1-1-11. Publ. CNEXO.

PREISENDORFER. R. W. 1961. Application of radiative transfer theory to light measurements in the sea, p. 11–29. *In* Radiant energy in the sea. Int. Union Geophys. Geod. Monogr. 10.

PRIEUR, L. 1976. Transfert radiatif dans les eaux de mer. Application à la détermination de paramètres optiques caractérisant leur teneur en substances dissoutes et leur contenu en particules. D.Sci. thesis, Univ. Pierre et Marie Curie. 243 p.

———, AND A. MOREL. 1975. Relations théoriques entre le facteur de réflexion diffuse de l'eau de mer à diverses profondeurs et les caractéristiques optiques, p. 278. [Abstr.] Int. Union Geophys. Geod. 16th General Assembly, Grenoble.

SMITH, R. C. 1973. Scripps spectroradiometer data, p. G1–G160. *In* SCOR Data Rep. Discoverer Expedition, v. 2. Scripps Inst. Oceanogr. Ref. 73-16.

SULLIVAN, S. A. 1963. Experimental study of the absorption in distilled water, artificial sea water, and heavy water in the visible region of the spectrum. J. Opt. Soc. Am. **53**: 962–968.

TYLER, J. E., AND R. C. SMITH. 1970. Measurements of spectral irradiance underwater. Gordon and Breach.

YENTSCH, C. S. 1960. The influence of phytoplankton pigments on the colour of sea water. Deep-Sea Res. **7**: 1–9.

Submitted: 9 August 1976
Accepted: 4 January 1977